VIROLOGICA SINICA

Electronic Supplementary Material

Longitudinal Characteristics of T Cell Responses in Asymptomatic SARS-CoV-2 Infection

Jingyi Yang[1,2#], Ejuan Zhang[1,2#], Maohua Zhong[1,2#], Qingyu Yang[2,3,4], Ke Hong[3,4], Ting Shu[2,3,4], Dihan Zhou[1,2], Jie Xiang[3,4], Jianbo Xia[6], Xi Zhou[1,2,3,7], Dingyu Zhang[3,4], Chaolin Huang[3,4]✉,You Shang[5,3,4]✉, Huimin Yan[1,2,7]✉

1 Joint Laboratory of Infectious Diseases and Health, Wuhan Institute of Virology & Wuhan Jinyintan Hospital, Wuhan Institute of Virology, Center for Biosafety Mega-Science, Chinese Academy of Sciences (CAS), Wuhan 430023 China
2 State Key Laboratory of Virology, Wuhan Institute of Virology, Center for Biosafety Mega-Science, CAS, Wuhan 430071, China
3 Center for Translational Medicine, Jinyintan Hospital, Wuhan 430023 China
4 Joint Laboratory of Infectious Diseases and Health, Wuhan Institute of Virology & Wuhan Jinyintan Hospital, Wuhan Jinyintan Hospital, Wuhan 430023 China
5 Department of Critical Care Medicine, Union Hospital, Tongji Medical College, Huazhong University of Science and Technology, Wuhan 430030 China
6 Department of Laboratory Medicine, Maternal and Child Health Hospital of Hubei Province, Tongji Medical College, Huazhong University of Science and Technology, Wuhan 430070 China
7 University of Chinese Academy of Sciences, Beijing 100049 China

Supporting information to DOI: 10.1007/s12250-020-00277-4

Supplementary materials and methods

Healthy donors

Eleven healthy age-matched male donors were enrolled as healthy controls, who were confirmed without ongoing or past SARS-CoV-2 infection.

SARS-CoV-2 infection detection and T cell responses evaluation

SARS-CoV2 infection was detected by qRT-PCR as described by our previous study (Cao et al., 2020) and by RBD-specific plasma IgM, IgG using colloidal gold strips.

Plasma and blood cells were separated from fresh peripheral blood from the SARS-CoV-2 infected case and healthy donors. Plasma was used for SARS-CoV-2 binding IgM or IgG detections. PBMCs were separated from the blood cells by density gradient centrifugation with human lymphocyte separation medium (DAKEWE, China) resuspended in complete RPMI1640 medium containing 10% FBS (Gibco), 1% penicillin and 1% streptomycin. PBMCs were then divided into three panels for analysis: panel 1 for T cell differentiation, proliferation and activation detection, panel 2 for T cell cytokine production detection, and panel 3 for Treg detection. PBMCs of panel 1 and panel 3 were directly used for staining while PBMCs of panel 2 were stimulated with 200 ng/mL PMA (Beyotime, China), 2.5 μmol/L ionomycin (Beyotime, China) in the presence of 1 μmol/L monensin (BioLegend, USA) and 2.5 μg/mL Brefeldin A at 37℃, 5% CO_2 for 4.5 h before staining. PBMCs were stained with dead cell discrimination marker (eBioscience™ Fixable Viability Dye eFluor™ 506, FVD) and surface-staining antibodies in PBS at 4℃ for 30 min. After washing with PBS, cells were fixed with fixation/permeabilization buffer (eBioscience) at 4℃ overnight, and then stained with the respective panel of intracellular markers in a permeabilization buffer at 4℃ for 30 min. Antibodies used for each panel were listed in table S2. A BD LSR Fortessa flow cytometer (Becton Dickinson) was used to assess the stained cells and data were analyzed using FlowJo V7.0.

Statistical analysis

Data analysis was carried out with InStat, version 5.0 (GraphPad Software, La Jolla, CA, USA) and the data of HD were presented as mean ± SD with dot plots.

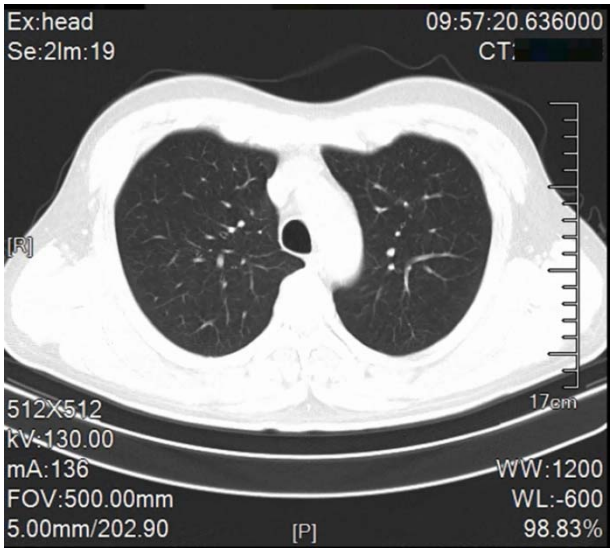

Supplementary Figure S1. Computed tomography of the chest of the patients with asymptomatic SARS-CoV-2 infection. Chest CT axial view lung window from the patient showing no significant abnormality on day 1 after admission to hospital.

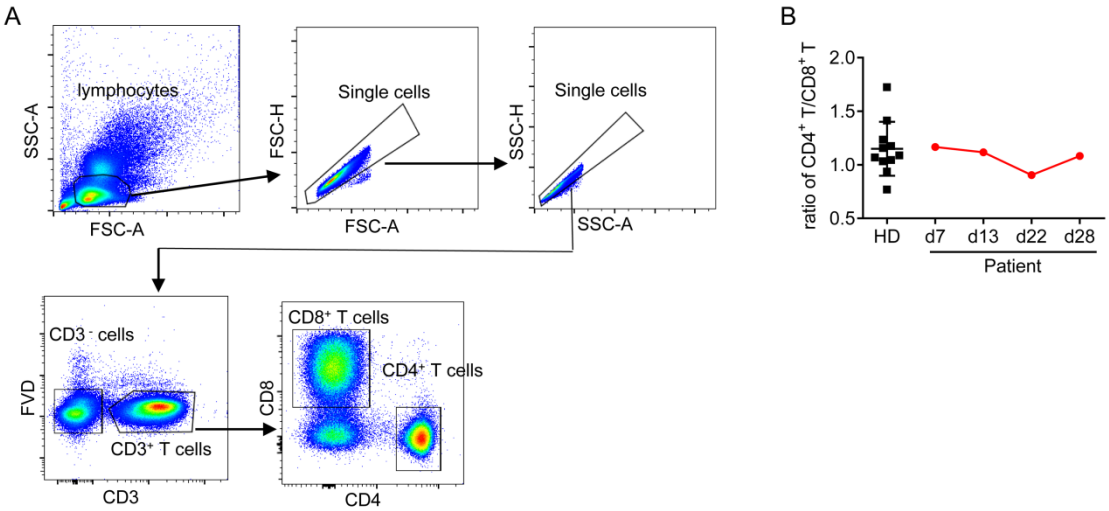

Supplementary Figure S2. Gating strategy of $CD4^+$ and $CD8^+$ T cells. **A**, Gating strategy of $CD4^+$ T cells, $CD8^+$ T cells in PBMC. **B**, the ratio of $CD4^+/CD8^+$ T cells in PBMCs of the patient at days 7, 13, 22 and 28 post hospitalization and in PBMCs of the healthy donors (HD, n=11).

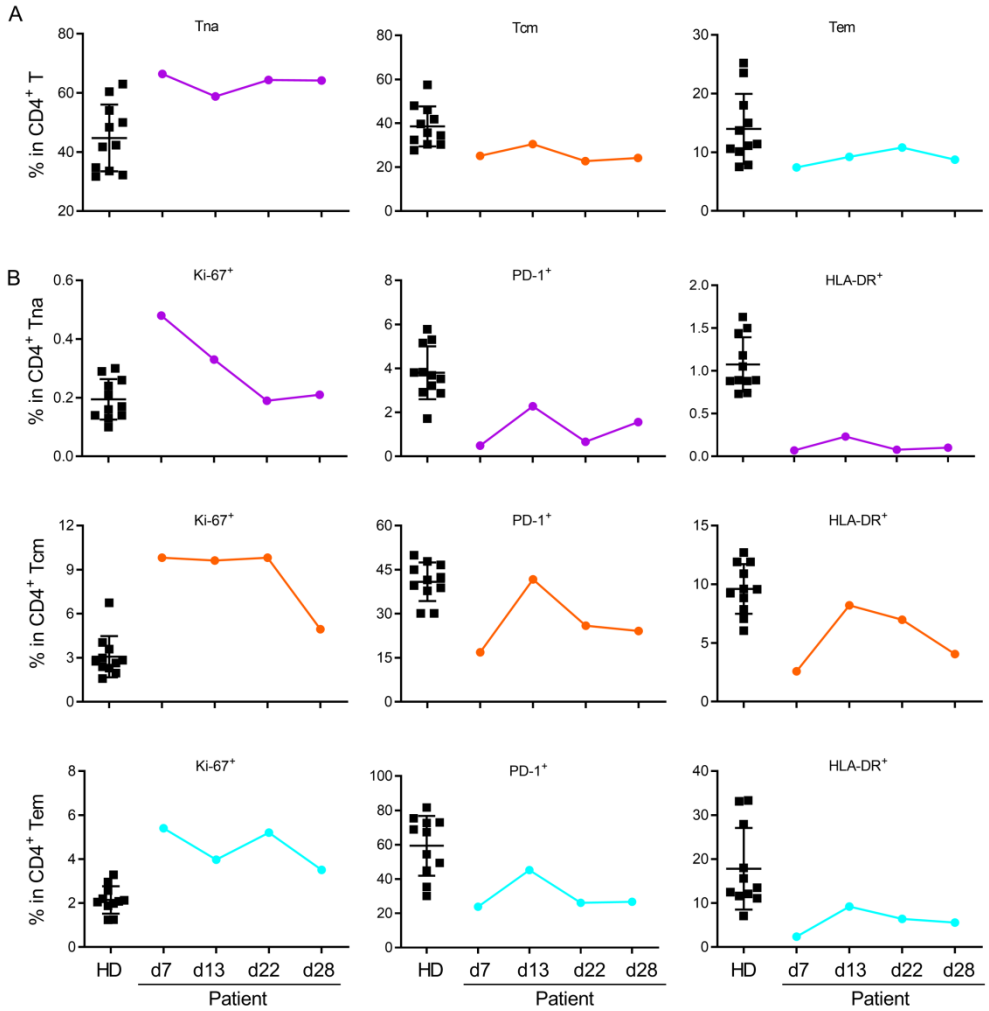

Supplementary Figure S3. Differentiation, proliferation and activation of the Tna, Tcm, Tem subsets of $CD4^+$ T cells.

A. Frequencies of naïve T cells (Tna), central memory T cells (Tcm) and effector memory T cell (Tem) subsets in the $CD4^+$ T cells. **B**. Frequency of Ki-67^+, PD-1^+ or HLA-DR^+ cells in Tna, Tcm, Tem subsets of $CD4^+$ T cells in PBMCs of the patient at days 7, 13, 22 and 28 post hospitalization and in PBMCs of healthy donors (HD, n=11).

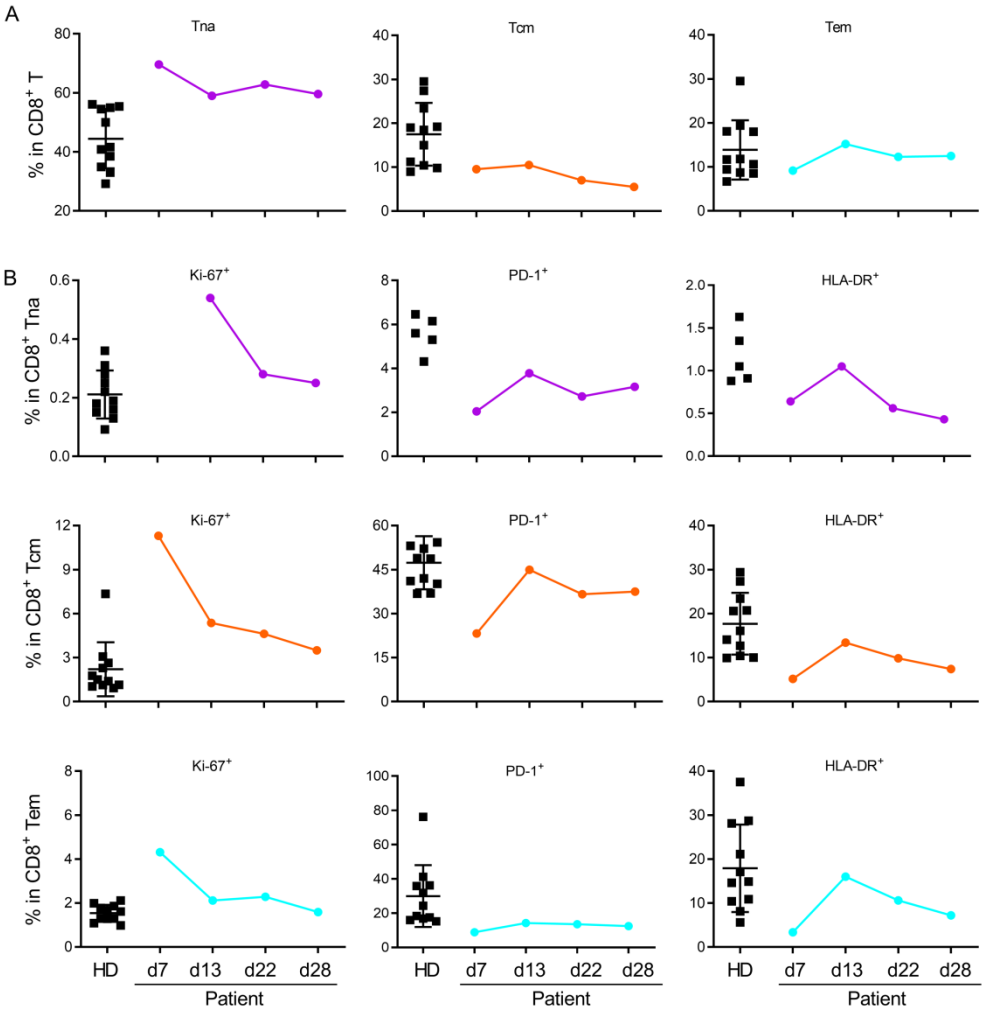

Supplementary Figure S4. Differentiation, proliferation and activation of the Tna, Tcm, Tem subsets of $CD8^+$ T cells. A. Frequencies of naïve T cells (Tna), central memory T cells (Tcm) and effector memory T cell (Tem) subsets in the $CD8^+$ T cells. B. Frequency of Ki-67^+, PD-1^+ or HLA-DR^+ cells in Tna, Tcm, Tem subsets of $CD8^+$ T cells in PBMCs of the patient at days 7, 13, 22 and 28 post hospitalization and in PBMCs of healthy donors (HD, n=11).

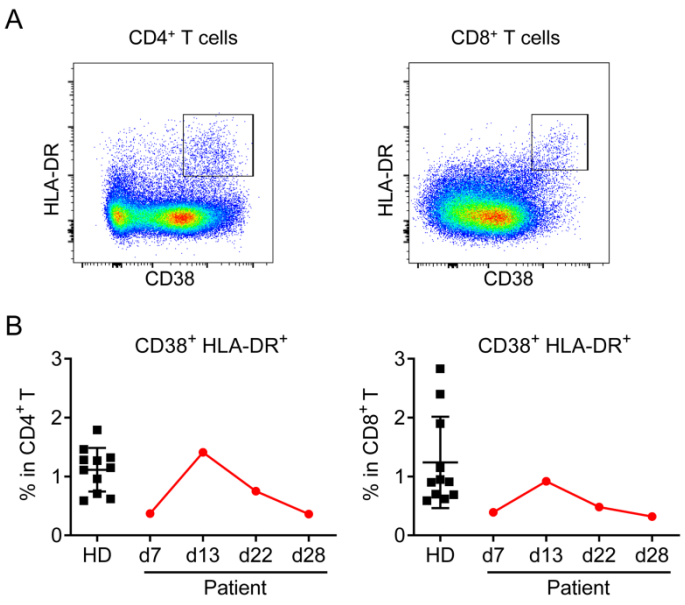

Supplementary Figure S5. The frequencies of $CD38^{+}HLA\text{-}DR^{+}$ cells in the $CD4^{+}$ and $CD8^{+}$ T cells. Gating strategy of $CD38^{+}HLA\text{-}DR^{+}$ activated cells. B. Frequencies of $CD38^{+}HLA\text{-}DR^{+}$ cells in $CD4^{+}$ and $CD8^{+}$ T cells of PBMCs detected in the patient at days 7, 13, 22 and 28 post hospitalization and in healthy donors (HD, n = 11).

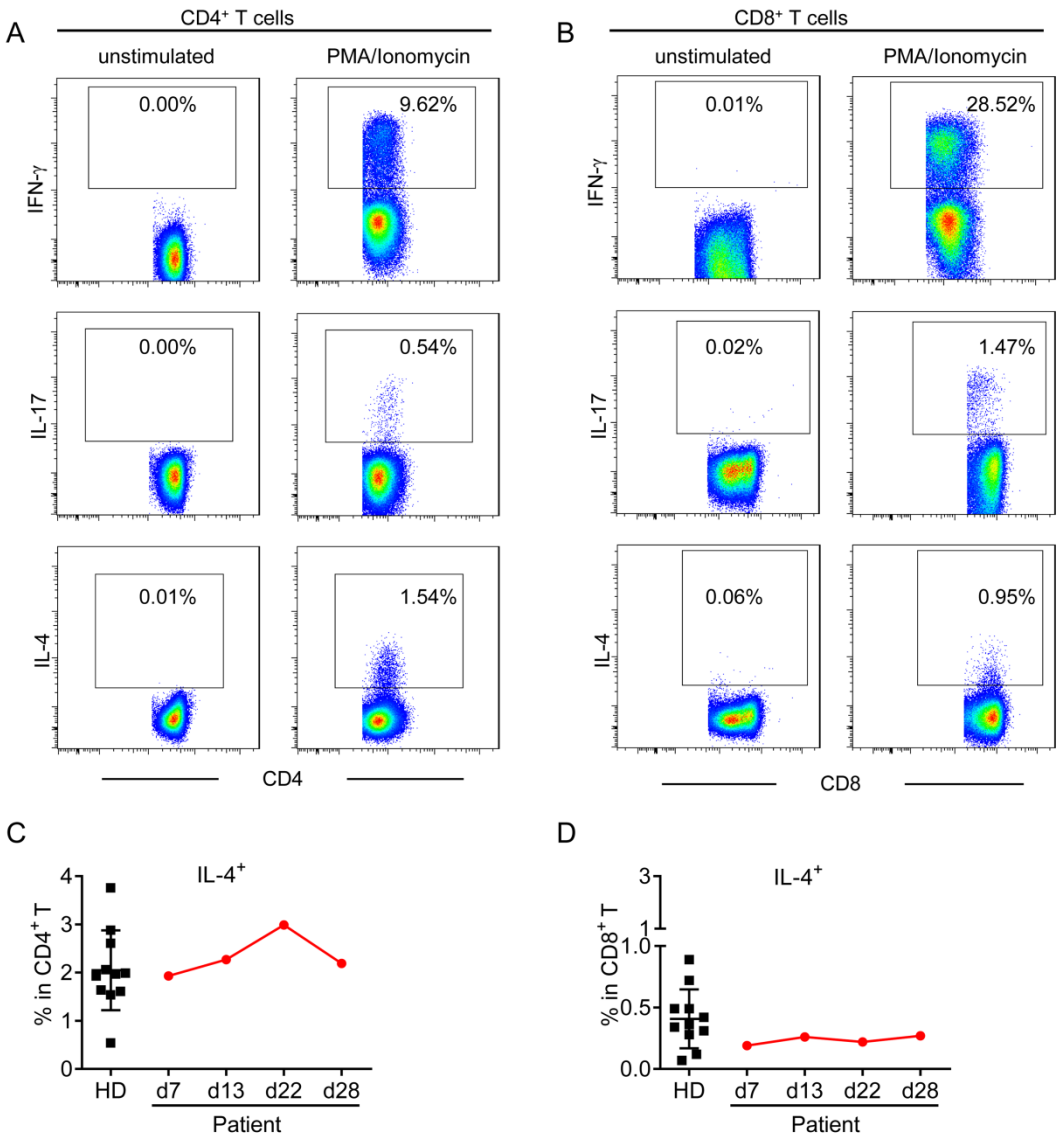

Supplementary Figure S6. Cytokine production of T cells in peripheral lymphocytes after *ex vivo* stimulation. PBMCs were isolated from the patient at days 7, 13, 22 and 28 post hospitalization and in healthy donors (HD, n=11). PBMCs were stimulated by PMA/Ionomycin for 4.5 h in the presence of BFA and monensin. The production of IFN-γ, IL-17, and IL-4 by CD4+ (A, C) or CD8+ T cells (B, D) were analyzed by intracellular cytokine staining and flow cytometry. IFN-γ, IL-4, and IL-17 producing CD4+ and CD8+ T cells were gated based on the unstimulated cells as shown in A and B.

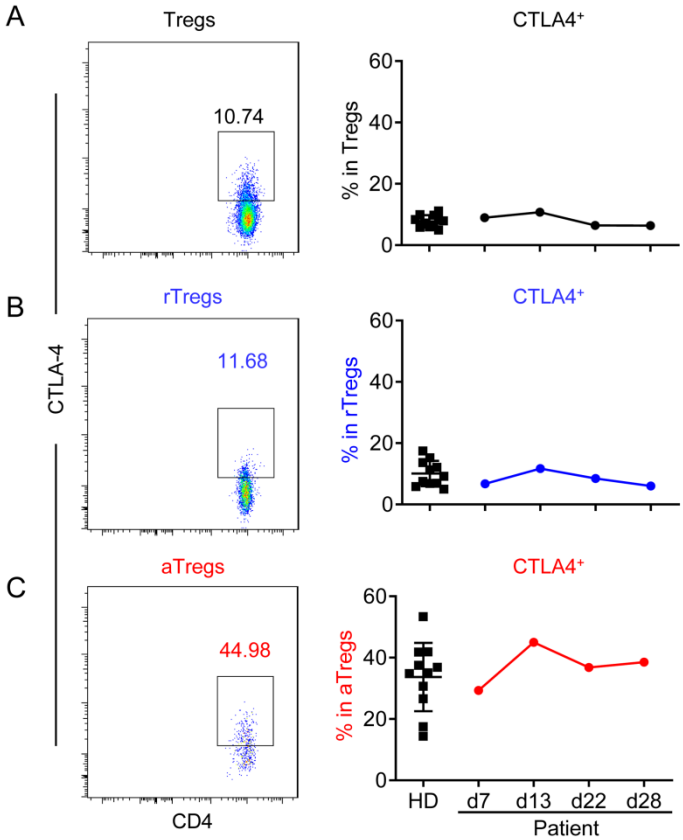

Supplementary Figure S7. The frequency of CTLA4$^+$ cells of Tregs and Treg subsets

Gating strategies and the frequencies of CTLA4$^+$ cells in Tregs (A) and its subsets: rTregs (B) and aTregs (C).

Supplementary Tables

Supplementary Table S1. Ct value of *N* gene, *E* gene, *RdRp* (R) gene of SARS-CoV-2 using qRT-PCR

Days post hospitalization	Ct value					
	Nasopharyngeal swab			Sputum		
	N	E	R	N	E	R
0	Pos	Pos	Pos			
1	34.4	38.1	37.6	19.6	23	22.6
2	20.5	20	20			
5	Neg	Neg	Neg			
8	Neg	Neg	Neg			
11	Neg	Neg	Neg	Neg	Neg	Neg
13	Neg	Neg	Neg	Neg	Neg	Neg
22	Neg	Neg	Neg	Neg	Neg	Neg
28	Neg	Neg	Neg	Neg	Neg	Neg

Supplementary Table 2: mAbs used in this study.

Panel	Antibodies (clone)	Staining procedure	Source	Identifier
1	Fixable Viability Dye eFluor™ 506	surface	eBioscience	65-0866-14
1	APC/Cyanine7 anti-human CD3 (HIT3a)	surface	BioLegend	300318
1	Alexa Fluor® 700 anti-human CD4 (OKT4)	surface	BioLegend	317426
1	Brilliant Violet 605™ anti-human CD8a (RPA-T8)	surface	BioLegend	301040
1	FITC anti-human CD45RO (UCHL1)	surface	BioLegend	304242
1	Pacific Blue™ anti-human CD27 (O323)	surface	BioLegend	302822
1	PerCP/Cyanine5.5 anti-human HLA-DR (L243)	surface	BioLegend	307630
1	Brilliant Violet 650™ anti-human CD38 (HB-7)	surface	BioLegend	356620
1	PE/Dazzle™ 594 anti-human CD279 (PD-1 (EH12.2H7)	surface	BioLegend	329940
1	PE anti-human Ki-67 (Ki-67)	intracellular	BioLegend	350504
2	Fixable Viability Dye eFluor™ 506	surface	eBioscience	65-0866-14
2	APC/Cyanine7 anti-human CD3 (HIT3a)	surface	BioLegend	300318
2	Alexa Fluor® 700 anti-human CD4 (OKT4)	surface	BioLegend	317426
2	Brilliant Violet 605™ anti-human CD8a (RPA-T8)	surface	BioLegend	301040
2	PE/Cy7 anti-human IL-4 (MP4-25D2)	intracellular	BioLegend	500824
2	PerCP/Cy5.5 anti-human IL-17A (BL168)	intracellular	BioLegend	512314
2	PE/Dazzle™ 594 anti-human IFN-γ (B27)	intracellular	BioLegend	506530
3	Fixable Viability Dye eFluor™ 506	surface	eBioscience	65-0866-14
3	Alexa Fluor® 700 anti-human CD3 (SK7)	surface	BioLegend	344822
3	Brilliant Violet 650™ anti-human CD4 (RPA-T4)	surface	BioLegend	300536
3	Brilliant Violet 605™ anti-human CD8a (RPA-T8)	surface	BioLegend	301040